A 3D IMAGE ANALYSIS METHOD FOR FIBROUS MICROSTRUCTURES: DISCRETIZATION AND FIBERS TRACKING

S. Le Corre[1*], P. Latil[2], L. Orgéas[2], P. J. J. Dumont[3], S. Rolland du Roscoat[2], C. Geindreau[2]

[1]LUNAM, LTN - CNRS, Université de Nantes, rue C. Pauc, BP 50609, Nantes, France
[2]Laboratoire 3SR, CNRS, Université de Grenoble, BP 53, 38041 Grenoble cedex 9, France
[3]Laboratoire LGP2, CNRS – Grenoble INP, 461 rue de la Papeterie, 38402 Saint-Martin d'Hères, cedex, France.

**steven.le-corre@univ-nantes.fr*

Keywords: fibrous media, discrete image analysis, fiber tracking, X-Ray microtomography.

Abstract:
The mechanics of fibrous materials is based on complex micro-mechanisms such as fiber motion, deformation, orientation and fiber-fiber contact interactions, which are generally difficult to characterize. To date, microstructural experimental data at the fiber scale are still scarce at this day, but the ongoing development of X-Ray micro-tomography opens the way to a much deeper understanding of such microstructural evolutions, *e.g*. during composite forming.
This work presents the founding principles of a 3D image analysis method, dedicated to fibrous and deformed materials. The challenge is double and consists in (i) developing an image processing tool able to individualize fiber-like objects in 3D images and (ii) following their motion at different stages of a macroscopic deformation process.
In order to set up clearly the basic analysis methods, we base on the use of virtual tomographies. Realistic fibrous networks are first obtained through a discrete simulation code based on molecular dynamics principles. They are then subjected to a macroscopic loading and at various deformation levels, each configuration being converted into a 3D binary image stack thanks to a ray-tracing technique. A perfect tomography is thus obtained, where all fibers are identified in the discrete code. Skeletonization algorithms are then applied, based on the use of a combination of distance map and thresholding procedures. Lastly, a discrete correlation procedure for the tracking of individual fibers is presented.

1 Introduction

In the past decades, the use of fiber-reinforced polymer composites in structural or functional applications has increased in various domains such as automotive or aerospace industries. Most of the fibrous reinforcements of such materials are made up of bundles containing few hundreds to few thousands of fibers. Composite materials exhibit multiple scales: the macroscopic part scale, the mesoscopic fiber bundle scale, and the fiber microscopic scale. During their processing, it is well known that the fibre bundles of these materials can be subjected to important displacements and deformations such as, for instance, orientation, consolidation, stretching, bending, twisting, shearing, bundle filamentation and breakage [2-8]. Such bundle mesoscale deformation mechanisms are induced both by the complex relative motions and the deformation of fibers at the microscopic level within the bundles. They

drastically affect the rheological behaviour of the composites during their forming by modifying, for instance, the permeability and several other properties [5, 9].
The X-ray microtomography technique which is now widely used in materials science is of particular interest for fibrous media such as composites since it can provide full 3D characterization of networks of fibers, even in composite materials with an optically opaque matrix. For instance, the orientation, the curvature, the compression and the breakage of discontinuous sized fiber bundles, occurring during compression moulding of an industrial SMC, were observed and quantified by using synchrotron X-ray microtomography [8]. Similarly, by performing with dry woven fabrics in situ shear and biaxial tests inside a laboratory X-ray microtomograph, Badel *et al.* [7] have underlined the great shape and surface changes of the cross sections of continuous fiber bundles of deformed textile reinforcements could be subjected to.
In a recent paper, Latil *et al.* [2] proposed an image analysis treatment able to automate the identification of individual fibers in a unidirectional structure. Many interesting results can be obtained from this tool in order to deeply analyze the microstructure, but it was only applied to a particular situation and few validations of the analysis were available. Furthermore, it is not possible to follow fibers from one reference configuration to a deformed one so that kinematic analyses are still not possible. Extending this work, we propose to improve those lacks by the use of numerical simulations and propose both the use of the notion of virtual tomography and fiber shape correlation.

2 Methods

2.1 Discrete simulation and virtual tomogaphy

When developing such a 3D analysis tool, one has to face many experimental constraints that can lead to a limited image quality (limited resolution, noise, poor contrast). Real images are imperfect, which adds a great complexity to the design of our discrete analysis procedure. Motivated by the need to get perfectly controlled 3D images, a discrete simulation code was developed based on molecular dynamics principles. In this first step, the objective is not to perform realistic mechanical analysis. We only want to generate and deform idealized fibrous microstructures, with the minimum requirement of generating hard-core microstructures, that is to say without interpenetration between touching fibers.

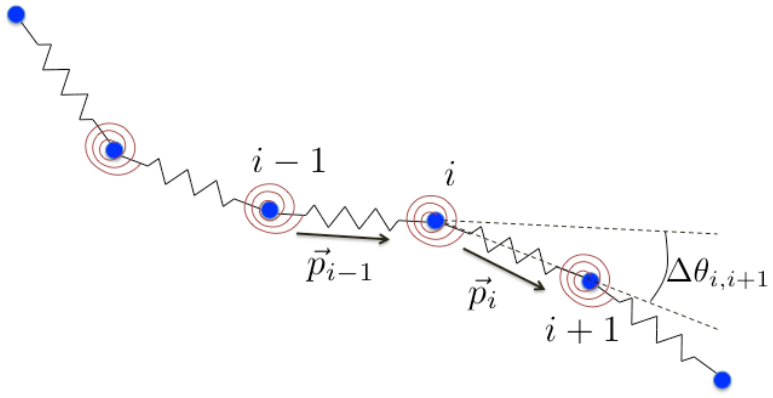

Figure 1: Molecular dynamics for fibers beam behavior.

In this approach, fibers are considered to have a circular cross section of diameter d_0. Fibers are discretized into segments of arbitrary length, and the equivalent Bernoulli beam model is modeled by defining a set of points linked by both tensile and bending forces (see figure 1). These forces are more simply defined by means of potentials which read respectively:

$$E_{tens} = \tfrac{1}{2} k_t \left(\left\| \vec{x}_{i+1} - \vec{x}_i \right\| - L_{seg}^{i,i+1} \right)^2 \quad (1)$$

and

$$E_{bend} = \tfrac{1}{2} k_b \left(\Delta\theta_{i,i+1} \right)^2 = \tfrac{1}{2} k_b \left(\mathrm{a}\cos\left(\vec{p}_{i-1} . \vec{p}_i \right) \right)^2 \quad (2)$$

where k_t and k_b denote the tensile and bending stiffness respectively. Contact forces are introduced in an approximate way by a penalization technique. When a contact between two segments is detected, the penetration δ is computed and a force $\vec{f}_{ij}^{\,C}$ is applied on both fibers along the normal vector to the contact plane $\vec{n}_C$ at the contact point:

$$\vec{f}_{ij}^{\,C} = -\chi(\delta)\, \vec{n}_C \quad (3)$$

In this last equation, $\chi(\delta)$ is the penalization law that can be chosen arbitrarily. In this work, we chose a Hertzian form of this law such as $\chi \propto \delta^{3/2}$.
Newton's equations of motion of points are then integrated in time using a standard Verlet, two-step algorithm. It is known for being energy conservative when no physical dissipation is introduced. Nevertheless, such a technique requires rather small time steps in order to respect the stability criterion. It is governed here by the tensile stiffness.
In order to generate 3D binary images from numerical discrete microstructures, a technique inspired by computer graphics (rasterisation) [6] was developed. Slices of the image stack were generated by computing the intersection of horizontal planes with fiber cylindrical segments. This enables to determine which pixels of the image grid have to be given a value of 1. Another technique, based on the use of ray-tracing was also envisaged, through the use of PovRay freeware, but proved to be much more time-consuming than the simple intersection calculation.

2.2 Skeletonization of tomography images

The skeletonization algorithm used in this work is similar to the one detailed in Latil *et al* [2], except that no watershed technique was used to separate the fibers in the binary image.
Briefly, the 3D distance map was computed with a standard routine like that proposed in the AVIZO software and objects were separated by a simple threshold on this map. After this separation step, centerlines of fibers could be computed. The noise on centerlines was then reduced by applying an average weighted filter. Those treatments finally enabled a quantitative analysis of the microstructure geometry, orientation, and of the number and geometry of fiber-fiber contacts.

2.3 Fiber tracking during deformation

The other challenge of this 3D image analysis work was also to be able to follow fibers' local motion during loading. Coupled with macroscopic loading and displacements measurements, such a tool will provide a much deeper understanding of micro-mechanisms of the overall deformation process of the fiber network. Conversely to usual field analysis techniques such as image correlation techniques, where the similarity of two zones of the reference and deformed images have to be quantified by appropriate correlation measures [10], we have taken advantage here of the discrete and linear nature of fibers to define a simple *pair selection criterion* for finding the fiber *j* in a deformed configuration corresponding to the considered fiber *i* in the reference configuration. Unlike the approach adopted for granular materials by Hall *et al* [11], it was checked that the criterion based on center of mass distance and rigid body motions was insufficient in many cases, whereas the basic point-to-point distance was the best

for fiber-like particles. The proposed pair selection criterion, illustrated in figure 2, was therefore defined as:

$$d_{ij} = \int_0^1 \left\| \vec{x}_i(s) - \vec{x}_j(s) \right\| ds \tag{4}$$

where d_{ij} is the integral of the distance between each point of the considered fibers, and s is a curvilinear abscissa, normalized with respect to the fiber length, which enables to compare fibers of different length. s is defined as:

$$s = s'/L \tag{5}$$

s' being the real curvilinear abscissa and L the considered fiber length. To prevent from a misorientation of s, one naturally has to compute d_{ij} with 1-s instead of s for one fiber and retain the smallest value. In principle, for one fiber i of the reference configuration, all the fibers j of the deformed configuration have to be tested but computations can be strongly accelerated by an appropriate thresholding, based, for example, on center of mass distance or on the fibers lengths.

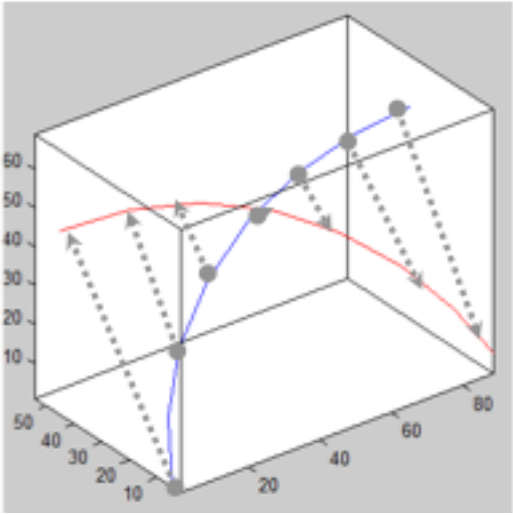

Figure 2 : Pairs selection criterion based on the point-to-point distance between two fibers.

3 Results

3.1 Simulation case

In this paper, we discuss the case of a compression of a set of fibers with an initial random 3D distribution in space and orientations. 50 fibers of length 25mm and diameter 1mm were generated into a square box of initial dimensions 25x25x25mm^3, which corresponds to an initial volume fraction of 6%. They were discretized into 11 segments, which leads to a problem of 550 degrees of freedom and enables rather fast computations. Walls of the box are assigned a repulsive potential, similar to that adopted for contact forces (3), which enables to maintain fibers inside the box all along the simulation. After the random generation step, fibers are generally not entirely inside the box, so that one has to wait a certain duration for the structure to be equilibrated before launching the box deformation. Once this initialization is performed, one length of the box is reduced at a constant speed of 1 m.s^{-1}. As visible from figure 3, the simulation can be run up to high compaction rate (about 80% shere), which corresponds to a final volume fraction of about 30%. Fiber maximum interpenetration is maintained to a reasonable level except in the end of the simulation, where contact forces become predominant.

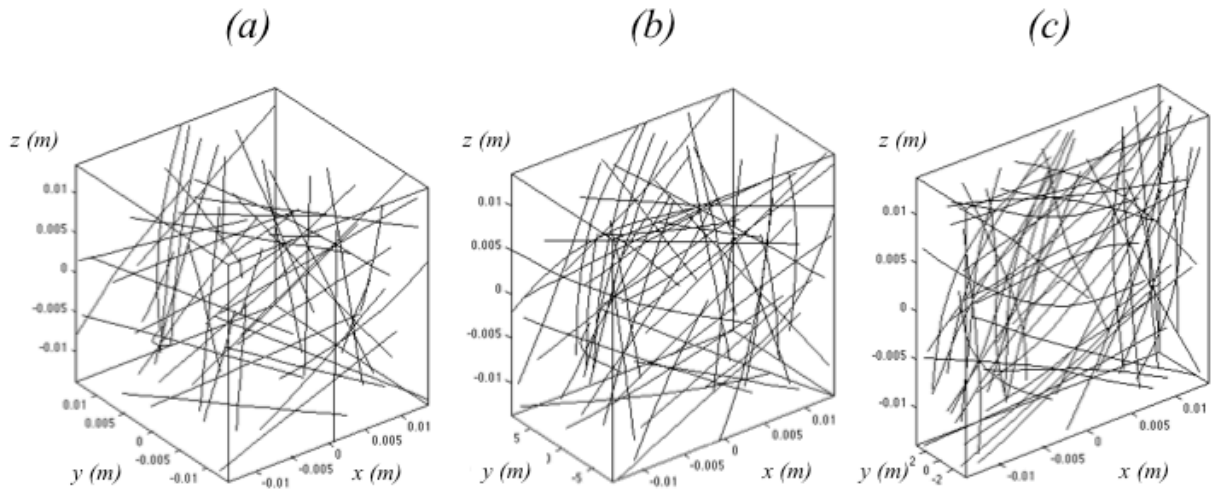

Figure 3: View of the numerical generated fiber networks of 50 fibers of 11 segments deformed in compression at different levels of height reduction: 0% *(a)*, 40% *(b)* and 80% *(c)*.

Then using the discrete fibers configurations at certain time steps, the virtual tomography technique described in section 2.1 was used to create 3D binary images as the one presented in figure 4. Images were generated for two cases of resolution: 10 and 20 pixels per diameter, which in practice represents an average and a good experimental resolution.

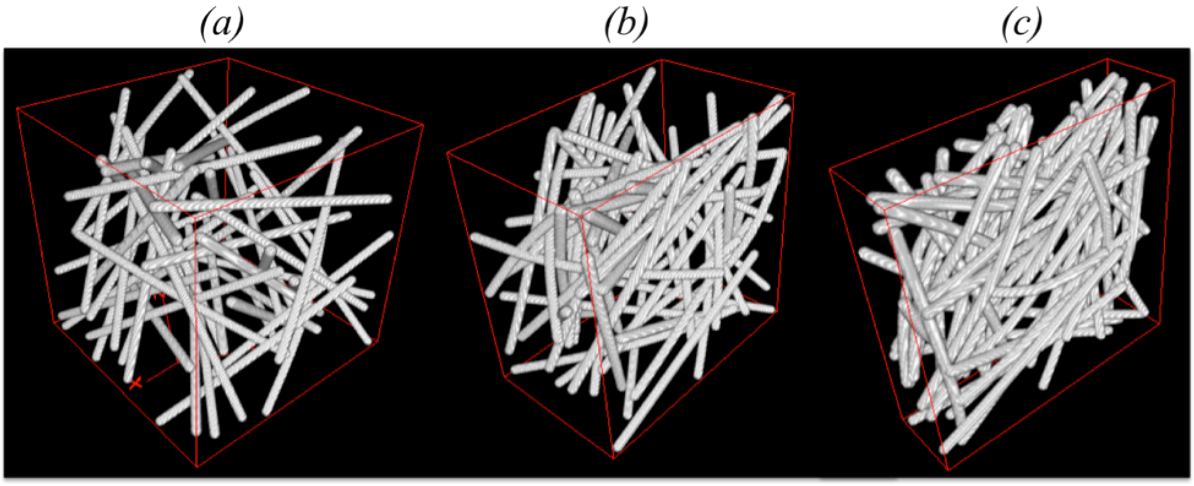

Figure 4: View of the reconstructed virtual tomograhies obtained from numerical fiber networks with a resolution of 10 pixels per diameter and at different levels of height reduction: 0% *(a)*, 40% *(b)* and 80% *(c)*.

3.2 Effects of the image analysis treatments.

After skeletonization , the aspect of the initial microstructure is entirely recovered as visible on figure 5. The general aspect is qualitatively good though some differences can be observed. Fibers centerlines are slightly shifted by the thresholding on the distance map but this effect is random and the average centerline is respected. We can also sometimes notice a “end effect” of the image treatment on fibers ends which should certainly be improved.

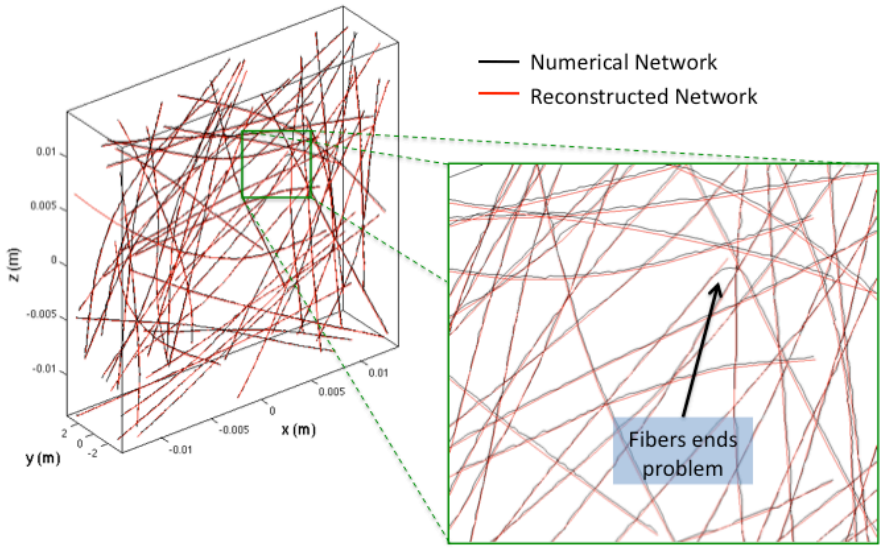

Figure 5: Analysis of the effect of the skeletonization on the recovery of the initial fibrous network, compression rate of 80%, resolution of 10 pixels per diameter.

When considering the locations of contact points between fibers, figure 6 shows rather important differences between the contact points detected by the simulation code and those obtained by the specific procedure proposed by Latil *et al.* [2]. The latter clearly finds a much higher number of contacts. Two reasons can explain such a discrepancy. First, the resolution affects the precision and can make that close enough fibers are found in contact. In this idea, most of the found contact points are not significant. But this should actually have a minor effect. Secondly, in practice, the numerical penetration allowed by code was sometimes very important which leads to large errors in the "experimental" contact determination. This can explain the poor apparent behavior of the method, but in this case, the problem probably comes from the simulations.

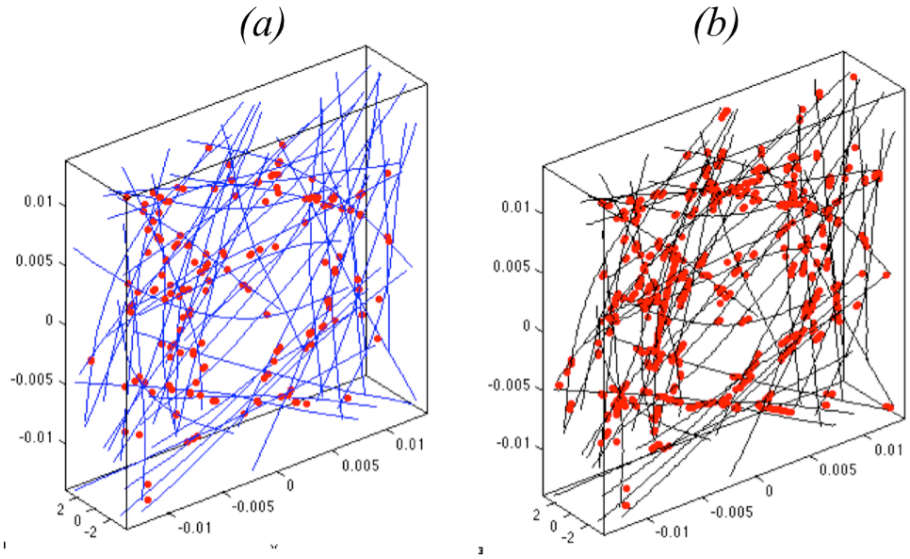

Figure 6: Contact point determined by the numerical simulation *(a)* compared to the ones obtained by the image analysis tool *(b)*, compression rate of 80%, resolution of 10 pixels per diameter.

3.3 Fiber tracking

The discrete correlation presented in 2.3 was also investigated thanks to the numerical results of the same test case, both for purely numerical results and for the "experimental" ones obtained from the virtual tomographies. Figure 7 presents a rate of correct pairs associations in terms of the compression rate, that is to say the level of deformation. For numerical networks, checking the correctness of results is very easy because fiber numbers are perfectly known. For "experimental" ones, we do not have such a reference so we use an indirect criterion. If the same pair is found performing the correlation from the reference to the deformed configuration and in the other direction, the relation is bilateral and we assume that the association is correct. As evident from figure 7, the numerical case shows excellent results. We get 98% of good correlations up to 40% of height reduction. If correlations are performed from one deformed state to another, we show that results are perfect along the deformation when using a difference of 10% of macroscopic deformation, and stays above 98% up to a difference of 20% deformation between the successive images.
Because of the treatment errors discussed in 3.2, correlations on "experimental" results are slightly poorer but the same trends are obtained and progressive correlations give about 90% of good results for a difference of 20% deformation between the successive images.

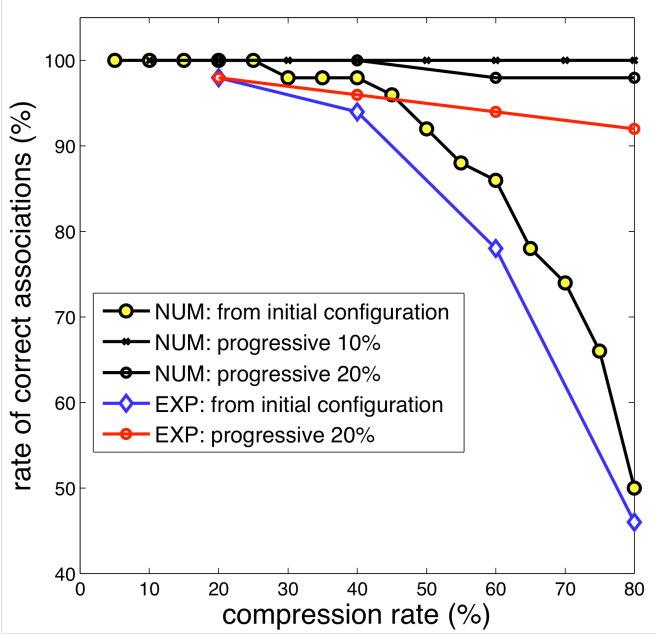

Figure 7: Analysis of the fiber tracking technique.

4 Conclusions

This paper presents several new ideas oriented towards the development of a robust and automatized 3D image analysis tool dedicated to fibrous media. We first discuss the principle of the virtual tomography to generate perfect test cases for the image analysis technique. Nevertheless, much care should be taken on the physics of the simulation tool, non physical situations with too much fiber interpenetration lead to erroneous results. In a second step, we also propose a rather simple fiber correlation technique that seems to work pretty well and theoretically enables to track fibers between images that differ by a macroscopic deformation of 20 up to 40% which is much higher than in standard image correlation techniques. This result was also confirmed on reconstructed fiber networks, after the image analysis treatment.

References

[1] Breen D., Mauch S., Whitaker R. 3D scan conversion of CSG models into distance, closest-point and color volumes. *Proceedings of volume graphics* (2000), pp. 135–158 (2000)
[2] P. Latil, L. Orgéas, C. Geindreau, P.J.J. Dumont, S. Rolland du Roscoat, "Towards the 3D in-situ characterization of deformation micro-mechanisms within a compressed bundle of fibres" Composite Science and Technology, **71**,pp. 480-8 (2011).
Robitaille F, Gauvin R. Compaction of textile reinforcements for composites manufacturing. i: Review of experimental results. Polym Compos, **19**,pp. 198–216 (1998).
[3] Buet-Gautier K, Boisse P. Experimental analysis and modeling of biaxial mechanical behavior of woven composite reinforcements. Exp Mech, **41**, pp. 260–269 (2001)
[4] Bickerton S, Buntain M, Somashekar A. The viscoelastic compression behavior of liquid composite molding preforms. Compos Part A, **34**, pp. 431–44 (2003)
[5] Comas-Cardona S, Le Grognec P, Binetruy C, Krawczak P. Unidirectional compression of fibre reinforcements. Part 1: A non-linear elastic-plastic behaviour. Compos Sci Technol pp. **67**, pp. 507–514 (2007).
[6] Dumont P, Vassal J-P, Orgéas L, Michaud V, Favier D, Månson JA-E. Processing, characterization and rheology of transparent concentrated fibre bundle suspensions. Rheol Acta, **46**, pp. 639–651 (2007).
[7] Badel P, Vidal-Salle E, Maire E, Boisse P. Simulation and tomography analysis of textile composite reinforcement deformation at the mesoscopic scale. Compos Sci Technol, **68**, pp. 2433–2440 (2008).
[8] Le TH, Dumont P, Orgéas L, Favier D, Salvo L, Boller E. X-ray phase contrast microtomography for the analysis of the fibrous microstructure of SMC composites. Compos Part A, **39**, pp. 91–103 (2008).
[9] Loix F, Badel P, Orgéas L, Geindreau C, Boisse P. Woven fabric permeability: from textile deformation to fluid flow mesoscale simulations. Compos Sci Technol, **68**, pp 1624–30 (2008).
[10] Leclerc H, Perie J-N , Roux S, Hild F. Voxel-Scale Digital Volume Correlation. Experimental Mechanics, **51**(4), pp. 479-490 (2011).
[11] Hall S, Bornert M, Desrues J, Pannier Y, Lenoir N, Viggiani G, Bésuelle P. Discrete and Continuum analysis of localised deformation in sand using X-ray CT and Volumetric Digital Image Correlation. Géotechnique **60**(5), pp 315-322 (2010).